Optimal Resource Allocation for Secure Multi-User Wireless Powered Backscatter Communication with Artificial Noise

Pu Wang*†, Ning Wang†, Monireh Dabaghchian†, Kai Zeng† and Zheng Yan*‡
*School of Cyber Engineering, Xidian University, Xi'an, China 710071
†Department of Electrical and Computer Engineering, George Mason University, Fairfax, VA, US 22030
‡Department of Comnet, Aalto University, Espoo, Finland 02150
Email:{pwang20, nwang5, mdabaghc, kzeng2}@gmu.edu, zyan@xidian.edu.cn

***Abstract*—In this paper, we consider a wireless powered backscatter communication (WPBC) network in which a full-duplex access point (AP) simultaneously transmits information and energy signals by injecting artificial noise (AN) to secure the backscatter transmission from multiple backscatter devices (BDs). To maximize the minimum throughput and ensure fairness and security, we formulate an optimization problem by jointly considering the power splitting ratio between dedicated information signals and AN, backscatter time and signal power allocation among multiple BDs. For a single BD network, we obtain a closed-form solution and evaluate its validity through proof-of-concept experiments. For the general case with multiple BDs, we present an iterative algorithm by leveraging block coordinate descent (BCD) and successive convex approximation optimization to solve a non-convex problem incurred in WPBC. We further show the convergence of the proposed algorithm and analyze its complexity. Finally, extensive simulation results show that the proposed algorithm achieves an optimal and equitable throughput for all BDs, and our work provides a good perspective of resource allocation to improve the performance of WPBC networks.**

I. Introduction

Simultaneous wireless information and power transfer (SWIPT) has emerged as a promising technology to prolong the lifetime of IoT devices that can harvest energy from radio frequency (RF) signals. But the harvested energy is limited and may not be enough for active RF transmission. Backscatter communication can be a supplement due to its ultra-low power consumption [1]. It enables the IoT backscatter devices (BDs) to transmit data by reflecting and modulating incident RF signals without any costly and power-hungry RF transmitters [2]. By seamlessly synthesizing SWIPT and backscatter communication, wireless powered backscatter communication (WPBC) networks was proposed to enable bi-directional communication between full-duplex access points (APs) and backscatter devices (BDs) [3]. In such a system, APs are devoted to power the entire network and communicate with all BDs. In addition, the RF signals of APs can be designed to improve the efficiency of energy harvesting and to secure backscatter transmission with physical layer security techniques, such as injecting artificial noise [4]. Furthermore, the uplink transmission of multiple BDs should be scheduled by APs to avoid co-channel interference and at the same time to meet throughput requirements. The key requirements of WPBC networks, such as energy efficiency and secure communication, are difficult to meet for all BDs in practice.

Most existing research on WPBC focuses on waveform design for making a tradeoff between harvested energy and backscatter communication [3]. For instance, beamforming is designed based on channel state information (CSI) to maximize total harvested energy with backscatter rate constraints [5]. But there are only a few works on resources allocation in a WPBC network, which is a crucial issue to improve network performance. Some authors investigated and analyzed the performance of system transmission in WPBC networks only with backscatter time and reflection ratio of each BD [6], [7]. However, the reflection ratios of BDs can not be arbitrary optimized in the overall network, since they are determinate when the BDs have been deployed in reality. Thus, for a practical WPBC network, there is an urgent need to fundamentally analyze and improve its performance. Besides, securing backscatter communication as another key issue has not been considered in the past, which could lead to data interception and privacy breaches. Because of the dynamic nature of the backscatter communication and location of BDs, the energy consumption, transmission requirements and security demands will vary accordingly. Thus, how to optimize the performance of the WPBC network, by overall considering the total power and time allocation and security requirements, remains a challenge.

In this paper, we consider a full-duplex WPBC network that consists of multiple BDs and a full-duplex AP with two antennas for simultaneous signal transmission and reception. The AP transmits information and energy signals that consist of the dedicated information signals to facilitate energy harvesting and artificial noise to improve the secrecy capacity of uplink channel. At the same time, all BDs alternately perform backscatter transmission in a time-division multiplex access manner. To improve the performance and ensure fairness of the WPBC network, an optimization problem is formulated to maximize the minimum throughput of all BDs, by jointly optimizing the backscatter time and power allocation and split-

ting ratio for artificial noise, subject to harvested energy and security constraints which is provided by injecting artificial noise.

Specifically, our main contributions are summarized as follows:

- We formulate an optimization problem to maximize the minimum throughput by jointly considering resource allocation together with requirements on harvested energy and security in a multi-BDs WPBC network.
- For a single-BD system, we theoretically obtain its solution, and then evaluate its validity and performance with proof-of-concept experiments.
- For a multi-BDs system, we propose an iteration algorithm by leveraging block coordinate descent (BCD) and successive convex approximation (SCA) optimization. We also prove its convergence and analyze its complexity.
- Numerical results show that an optimal throughput for all BDs can be achieved, as compared to equal resource allocation. Our work also can provide a good perspective of system performance for selecting an appropriate resources allocation policy.

The rest of the paper is organized as follows. We introduce the related work in Section II. A system model and a max-min optimization problem are given in Section III. Section IV analyzes the resource allocation of the single BD system and provides the proof-of-concept experimental results. An iterative algorithm to solve the problem for a multi-BDs WPBC system is proposed in Section V. In Section VI, the numerical experimental results are presented to verify the performance of the proposed joint design. Finally, Section VII concludes the paper.

II. Related Work

One of key challenges of SWIPT systems is optimal signal waveform or beamforming design to maximize the signal-to-noise ratio (SNR)-energy region. The non-linearity of the rectifier at energy-harvesting devices and the frequency diversity gain were mostly exploited to design the signal waveforms [8], [9]. For the secure downlink transmission in WIPT networks, the secure signal waveforms were designed based on the CSI to enhance the secrecy capacity in a fading wiretap channel [10], [11]. In addition, energy beamforming and/or artificial noise are another way to achieve confidential communication by being utilized to jam eavesdroppers, because they can be canceled at legal receivers [12].

Backscatter communication is different from traditional wireless communication, because it does not require any active RF components. So it can be applied in the SWIPT systems to further reduce power consumption. Han and Huang [3] applied stochastic geometry to model and analyze the coverage and capacity of a WPBC network. In [7], the authors investigated an ambient backscatter communication network without a dedicated AP and analyzed its performance on backscatter time and reflection ratio of BDs. But the reflection ratios of BDs cannot be optimized in the overall problem, since they are determinate when the BDs have been deployed in the network. In addition, backscatter communication can be easily eavesdropped by illegal users because of its open nature [13]. Its security is still facing a big challenge, especially for the limited computational and energy resources of BDs, where complicated encryption algorithms may not be afforded and thus impossible to be applied [14]. One promising direction is to apply physical layer security mechanisms, such as adding artificial noise, to defend against eavesdropping. But in WPBC networks, the utilization of artificial noise will reduce the efficiency of energy harvesting and backscatter transmission [8]. Therefore, for a multi-BDs WPBC network, on the one hand, we utilize artificial noise to secure the backscatter transmission of all BDs; on the other hand, with transmission resource constraints, we optimize network performance by jointly considering the power splitting ratio for artificial noise, transmission power and backscatter time allocation for all BDs.

III. System Model and Problem Formulation

We consider a WPBC network that consists of a full-duplex AP with two antennas, $N(N \geq 1)$ legitimate BDs, and one passive eavesdropper as shown in Fig. 1. The AP simultaneously transmits RF signals to all BDs and receives backscattered information. We are only interested in uplink transmission in which each BD transmits its data over the incident RF signals. Each BD contains a backscatter antenna, a switched load impedance, an information receiver, an energy harvester, and other modules (e.g., micro-controller, battery, sensors). Here, as typically considered in a backscatter system, we assume that the BDs are semi-passive devices that harvest energy from the RF signals of AP and store in a battery for subsequent circuit operations. During receiving backscatter signals from BDs, the AP needs to operate in a full-duplex mode to continuously transmit RF signals and power all BDs. The AP can perfectly separate its received signals from the transmitted signals, a common assumption in backscatter communication systems [15].

The channels are modeled as frequency-flat and quasi-static. Parameters h_k and g_k denote the channel gains of forward and backward channels between the AP and the k-th BD, respectively. We assume that each BD will backscatter the incident RF signals to the AP, so that the AP can obtain the full channel gain information. Let h_{ke} and denote h_{re} the channel between the k-th BD and the eavesdropper and the channel between the AP and the eavesdropper, respectively. We also assume that the AP can obtain the CSI of eavesdropper as in [16], which is widely adopted in the physical-layer security literature. Otherwise, the AP cannot get whole CSI of eavesdroppers,but it still can obtain the their statistics CSI, i.e, the CSI distribution of the eavesdropper.

For backscatter transmission, we consider a frame-based protocol as shown in Fig. 1. Each frame duration T (seconds) consists of N slots. The k-th slot with duration $\beta_k T$ is assigned to the k-th BD for backscattering communication and $\boldsymbol{\beta} = [\beta_1, \beta_2, ..., \beta_N]^T$ denotes the time vector for all BDs. The time vector needs to be appropriately allocated satisfy each

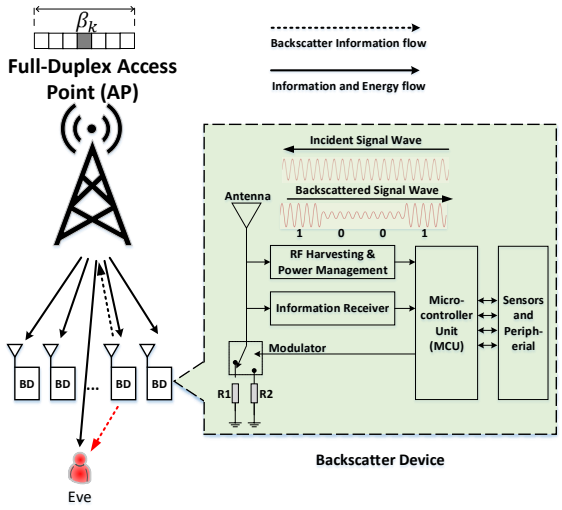

Fig. 1. Multiple access scheme in a WPBC network.

BD's throughput requirement, since different BDs may have different distances to AP.

To secure the transmission, the AP injects an artificial noise into the information signals to improve the secrecy capacity of the backscatter channel. The artificial noise is statistically identical to the additive white Gaussian noise (AWGN). The transmitted signals of AP to the k-th BD can be expressed as $w_k x + z_k$, where x, w_k, and z_k indicate the information-bearing signal, the dedicated information carrier, and the artificial noise, respectively. Without loss of generality, we assume that $\mathbb{E}(|x^2|) = 1$. The signal power allocated to k-th BD is denoted by P_k, where $P_{w,k} = \rho_k P_k (0 < \rho_k < 1)$ denotes dedicated carrier power and the remaining $P_{z,k}$=(1-ρ_k)P_k for artificial noise. $\mathbf{P} = [P_1, P_2, ..., P_N]^T$ and $\boldsymbol{\rho} = [\rho_1, \rho_2, ..., \rho_N]^T$ denote the power allocation vector and the power splitting ratio vector for all BDs, respectively.

The dedicated carrier is designed to facilitate energy harvesting with the nonlinear rectenna model at BDs, such as the power-optimized waveform (POW) described in [17], [18]. Let η_1 and $\eta_2 (0 < \eta_2 < \eta_1 < 1)$ be the energy-harvesting efficiency for the dedicated carrier and the artificial noise, respectively. When a BD is in backscatter communication, a proportion of the incident power is reflected backward. We assume the power reflection coefficient is $\mu (0 < \mu < 1)$ and the remaining part $(1-\mu)$ propagates to the energy harvester. According to the aforementioned protocol, the k-th BD will harvest the remaining part $(1-\mu)$ in the k-th slot, while scavenging all incident power of RF signals in other slots. Thus, the total energy harvested by the kth BD during all the slots is

$$E_k(\boldsymbol{\beta}, \boldsymbol{\rho}, \mathbf{P}) = \beta_k(1-\mu)(\eta_1 P_{w,k} + \eta_2 P_{z,k})|h_k|^2 + \sum_{i=1, i\neq k}^{N} \beta_i(\eta_1 P_{w,i} + \eta_2 P_{z,i})|h_k|^2, \quad (1)$$

where the first term indicates the energy harvested in the k-th slot and the last term for all other slots.

In the k-th slot, when the k-th BD backscatters the incident signals with its information symbol s, whose duration is much longer than the downlink symbol, the received signal at the AP is

$$y_k = g_k h_k \sqrt{\mu}(w_k x + z_k)s + g_k n_k + n_r, \quad (2)$$

where s has the same statistical characteristics of x , n_r is AWGN at the AP with power σ_r^2, and n_k is AWGN at the k-th BD with power σ_k^2 that will also be backscattered to AP.

In the equation above, the first term is the useful information signal and the remaining two terms constitute the combined AWGN noise. Note that z_k in Eq. (2) is the artificial noise that arrives at the AP after going through the round-trip propagation. It has unknown time and phase shifts caused by the signal propagation as well as the BD processing. Hence, it is difficult for the AP to recover the value of z_k without channel training and tracking. However, the artificial noise cancelation can be done via a standard signal processing technique with the fact that the AP has prior knowledge of the noise signal z_k. Nevertheless, there is still a possibility that AP can partially cancel this backscattered noise. We introduce an attenuation factor κ that indicates how successful the AP cancels the backscattered noise. But we note that in contrast to the AP, the eavesdropper faces more difficulty in performing a similar noise attenuation since it does not have any knowledge of the artificial noise. Given the noise injection described above, the SNR of the backscattered signal at the AP is given by

$$\gamma_{r,k} = \frac{\mu P_{w,k}|h_k|^2|g_k|^2}{\kappa\mu P_{z,k}|h_k|^2|g_k|^2 + |g_k|^2\sigma_k^2 + \sigma_r^2}. \quad (3)$$

Hence, the k-th BD's throughput normalized to the frame duration T is

$$R_{r,k}(\rho_k, \beta_k, P_k) = \beta_k \log(1 + \gamma_{r,k}). \quad (4)$$

Unfortunately, the dedicated carrier is known to the eavesdropper and hence, does not interfere with the eavesdropper's reception of the BD's backscatter signal. But the injecting noise at the AP is to create additional interference at the eavesdropper. So the signal received by the eavesdropper after removing the dedicated carrier directly from the AP is given by

$$y_k = h_{ke} h_k \sqrt{\mu}(w_k x s + z_k s) + h_{ke} n_k + n_e + h_{re} z_k, \quad (5)$$

where the last term is the artificial noise directly transmitted from the AP and n_e is the AWGN at the eavesdropper. Neither the directly injected noise nor the noise backscattered from the k-th BD is known to the eavesdropper. So the SNR of the received signals at the eavesdropper is given by

$$\gamma_{e,k} = \frac{\mu|h_k|^2|h_{ke}|^2 P_{w,k}}{[\mu|h_k|^2|h_{ke}|^2 + |h_{re}|^2]P_{z,k} + |h_{ke}|^2\sigma_k^2 + \sigma_e^2}. \quad (6)$$

From Eq. (6), the AP can limit the eavesdropper's SNR by controlling the injected noise power. Therefore, the achievable

secrecy rate between the AP and the k-th BD can be expressed as

$$\begin{aligned} C_k^s(\rho_k, P_k) = & \ [C_k^r - C_k^e]^+ \\ = & \ [\log(1+\gamma_{r,k}) - \log(1+\gamma_{e,k})]^+, \end{aligned} \tag{7}$$

where $[\cdot]^+ = \max(\cdot, 0)$.

Because of the "doubly near-far" problem [19], the AP will allocate more resources to close BDs than the far BDs, thus resulting in unfair performance among different BDs. Therefore, in order to maximize the minimum throughput with sufficient fairness, we formulate an optimization problem to jointly optimize backscatter time allocation and power assignment policy, while satisfying the requirements of the individual harvested energy and secrecy rate. This practical optimization problem can thus be expressed as,

$$\begin{aligned} \max_{\boldsymbol{\beta},\boldsymbol{\rho},\mathbf{P}} \quad & \min_{1\le k\le N} R_{r,k}(\rho_k, \beta_k, P_k) \\ \text{s.t.} \quad & C_k^s(\rho_k, P_k) \ge C_{th,k}, \quad k = 1, \ldots, N \\ & E_k(\boldsymbol{\beta}, \boldsymbol{\rho}, \mathbf{P}) \ge E_{th,k}, \quad k = 1, \ldots, N \\ & \sum_{k=1}^{N} \beta_k P_k \le \bar{P} \\ & \sum_{k=1}^{N} \beta_k = 1 \\ & 0 < \beta_k < 1, \quad k = 1, \ldots, N. \end{aligned} \tag{8}$$

where $\bar{P}$ indicates the sum-energy constraint of the AP normalized to the frame duration T, $C_{th,k}$ and $E_{th,k}$ are the requirements of lowest secrecy rate and lowest harvested energy, respectively.

Note that there are some conflicting goals in the above joint optimization problem. On the one hand, from the secrecy capacity point of view, according to Eq. (7), the injection noise at eavesdropper is desired to be as large as possible. However, it reduces the power for dedicated information signal that will decrease the transmission rate and lower the efficiency of energy harvesting. On the other hand, from the perspective of the resources allocation, by allocating longer backscatter time and more signal power, the throughput of backscatter can be improved. Hence, a suitable resource allocation policy should be selected with different application scenarios and requirements. But the non-convex problem in Eq. (8) is challenging to solve since the backscatter time allocation variables $\boldsymbol{\beta}$, power ratio allocation variables $\mathbf{P}$ and power splitting ratio variables $\boldsymbol{\rho}$ are all coupled in the non-convex objective function and the constraints of secrecy capacity and harvesting energy.

Before we proceed to solve the problem in Eq. (8), we first study its feasibility for given $E_{th,k} = 0$, where $k = 1, \ldots, N$. This reduces to the case of no energy constraint for none of BDs, while the signals $w_k x + z_k$ only convey information. Only considering the secrecy capacity [13], [20], positive secrecy capacity can always be achieved by injecting suitable artificial noise. Without loss of generality, in the rest of paper, we assume that our problem is feasible and secrecy rate is $C_k^s(\rho_k, P_k) = \log(1+\gamma_{r,k}) - \log(1+\gamma_{e,k})$.

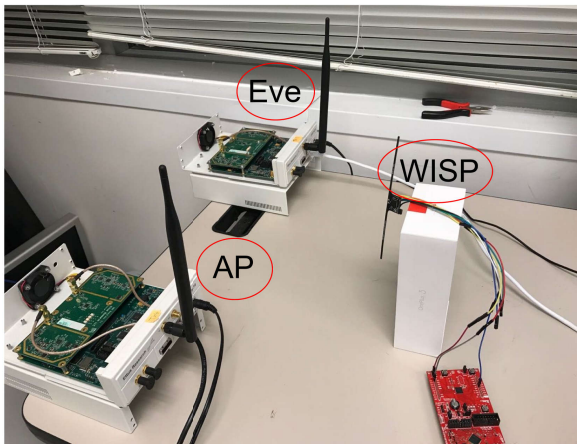

Fig. 2. Experimental set-up in the single-user WPBC network.

IV. Joint Resource Allocation in a Single-device WPBC Network

In this section, we consider a special case of Eq. (8) when there is only one BD in the WPBC system, i.e., $N = 1$, then, evaluate its validity through proof-of-concept experiments.

A. Solution for Single BD Case

For brevity, the subscript $k = 1$ is omitted in this section. The backscatter time vector $\boldsymbol{\beta}$, the transmission power vector $\mathbf{P}$ and the power splitting ratio vector $\boldsymbol{\rho}$ reduce to the constants $\beta = 1$, $P = \bar{P}$ and a scalar ρ, respectively. Optimization problem in Eq. (8) is then simplified as

$$\begin{aligned} \max_{\rho} \quad & R_r = \log(1+\gamma_r) \\ \text{s.t.} \quad & \log(1+\gamma_r) - \log(1+\gamma_e) \ge C_{th}, \\ & (1-\mu)(\eta_1 \rho P + \eta_2 (1-\rho) P)|h|^2 \ge E_{th}, \end{aligned} \tag{9}$$

where

$$\gamma_r = \frac{\mathrm{A}\rho}{\kappa \mathrm{A}(1-\rho) + D} = \frac{\mu |h|^2 |g|^2 P \rho}{\kappa \mu |h|^2 |g|^2 P (1-\rho) + |g|^2 \sigma^2 + \sigma_r^2},$$

$$\gamma_e = B \frac{\rho}{1-\rho} = \frac{\mu |h|^2 |h_{be}|^2 P}{[\mu |h|^2 |h_{be}|^2 + |h_{re}|^2] P} \frac{\rho}{1-\rho}.$$

We assume a worst-case scenario of no noise at the eavesdropper ($|h_e|^2 \sigma^2 = \sigma_e^2 = 0$). The objective function in Eq. (9) is a logarithm, which is concave and monotonically increases with ratio ρ, and all constraints only limit the interval of ρ, so the optimal value of R_r can be easily obtained at the maximum value of ρ.

B. Experimental Results of Single BD Case

In order to evaluate the validity and the performance of the single BD case, we implemented a single-BD WPBC system, as shown in Fig. 2. A USRP N210 was used as an AP that generates RF signals at the frequency of 900MHz and another USRP N210 as an eavesdropper, and a wireless identification and sensing platform (WISP) [21] is an ultra-low power passive UHF RFID tag as a BD. The WISP scavenges

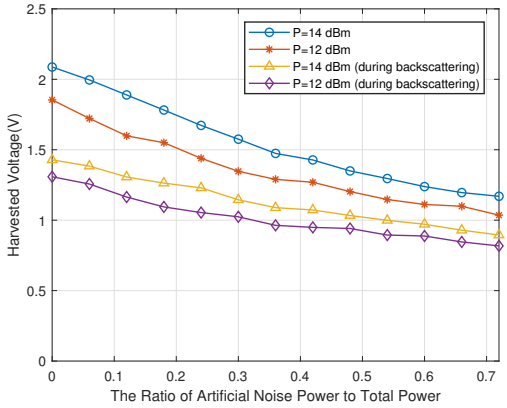

Fig. 3. Harvested voltage vs splitting ratio with transmission power.

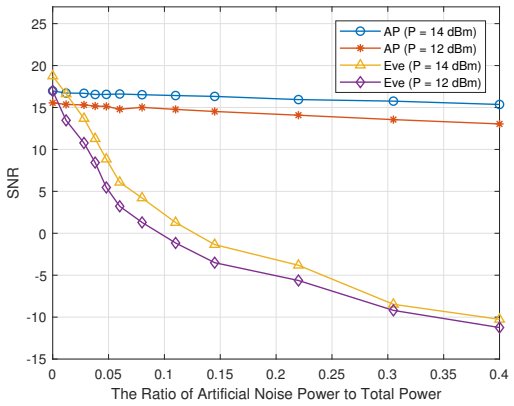

Fig. 4. SNRs of AP and Eve vs splitting ratio with transmission power.

energy from the RF signal and converts into DC voltage to power its circuit and backscatter transmission at a rate of 4 kbps. As the approach introduced above, we added artificial noise in the downlink RF signals to decrease the SNR at the eavesdropper. However, with the same total power emitted by AP, as the power used for artificial noise increases, the voltage at WISP will decrease, as well as the SNR at AP.

Therefore, we evaluate the voltage generated at the WISP, whether it is backscattering or not, and the SNRs of the signal received at both USRPs. Through the results in Fig. 3, the voltage at the WISP drops when increasing the proportion of noise power. In addition, the voltage harvested by the WISP declines about 36% while it is backscattering. Fig. 4 shows the SNR of AP and Eve versus the splitting ratio for the artificial noise.. Without artificial noise in the downlink signal, the SNR of the eavesdropper is higher than that of the AP's, because Eve is set closer to the WISP in our experiment. Thus, if the eavesdropper is close to the transmitter and has a very sensitive receiver as compared to the legitimate receiver, there is a grave risk of information leakage. But as the power of injected noise increases, the SNR of the eavesdropper reduces faster than the AP's. Therefore, positive secrecy capacity can be achieved by injecting a suitable power of artificial noise into the downlink signal

V. Joint Resource Allocation in a Multiple-BD WPBC Network

In this section, we consider the joint resource allocation in the WPBC system with multiple BDs. In general, there is no standard method for optimally and efficiently solving the non-convex optimization problem in Eq. (8). Hence, we propose an iterative algorithm to solve it sub-optimally by applying the block coordinate descent (BCD) [22] and the successive convex approximation (SCA) [23], [24]. Specifically, given the power allocation vector $\mathbf{P} = [P_1, P_2, \ldots, P_N]$ and power splitting ratio vector $\boldsymbol{\rho} = [\rho_1, \rho_2, \ldots, \rho_N]$ for all devices, we optimize the backscatter time vector $\boldsymbol{\beta} = [\beta_1, \beta_2, \ldots, \beta_N]$ by solving a linear programming; given the time allocation $\boldsymbol{\beta}$ and power allocation $\mathbf{P}$, we optimize the splitting ratio $\boldsymbol{\rho}$ by solving a multivariate non-coupling problem like in the single-BD WPBD system; given the time allocation vector $\boldsymbol{\beta}$ and splitting ratio $\boldsymbol{\rho}$, we optimize the power allocation $\mathbf{P}$ by utilizing the SCA-based method to approximately solve a non-convex problem. After presenting the overall algorithm, we prove its convergence and analyze its complexity.

A. Backscatter Time Allocation Optimization

At iteration $j (j \geq 1)$, given a power allocation vector $\mathbf{P}^j$ and a power splitting ratio vector $\boldsymbol{\rho}^j$, the backscatter time allocation vector $\boldsymbol{\beta}$ can be optimized by solving the following problem

$$\begin{aligned} \max_{\boldsymbol{\beta}} \quad & \min\ \beta_k \log(1+\gamma_{r,k}(e_k^j, P_k^j)) \\ \text{s.t.} \quad & C_k^s(\rho_k^j, {P_k}^j) \geq C_{th,k}, \quad k=1,\ldots,N \\ & E_k(\beta_k, \rho_k^j, P_k^j) \geq E_{th,k}, \quad k=1,\ldots,N \\ & \sum_{k=1}^{N} \beta_k P_k^j \leq \bar{P}, \\ & \sum_{k=1}^{N} \beta_k = 1. \end{aligned} \tag{10}$$

The problem can be converted to a reduced linear programming by introducing a slack variable [25], since constraint functions are all linear. It can be solved efficiently by existing optimization methods or tools, such as CVX [26].

B. Power Splitting Ratio Optimization

At iteration j $(j \geq 1)$, given a power allocation vector $\mathbf{P}^j$ and a backscatter time allocation vector $\boldsymbol{\beta}^j$, the power splitting ratio vector $\boldsymbol{\rho}$ can be optimized by solving the following problem

$$\begin{aligned} \max_{\boldsymbol{\rho}} \quad & \min\ \beta_k^j \log(1+\gamma_{r,k}(\rho_k, P_k^j)) \\ \text{s.t.} \quad & C_k^s(\rho_k, {P_k}^j) \geq C_{th,k}, \quad k=1,\ldots,N \\ & E_k({\beta_k}^j, \rho_k, P_k^j) \geq E_{th,k}. \quad k=1,\ldots,N \end{aligned} \tag{11}$$

For a given vector $\mathbf{P}^j$ and $\boldsymbol{\beta}^j$, the power splitting ratios for all BD are independent of each other. Thus, it can be decomposed

into N independent subproblems to optimize the ratio for each BD. The k-th subproblem is as

$$\begin{aligned} \max_{\rho_k} \quad & \beta_k^j \log(1+\gamma_{r,k}(\rho_k, P_k^j)) \\ \text{s.t.} \quad & C_k^s(\rho_k, {P_k}^j) \geq C_{th,k} \\ & E_k({\beta_k}^j, \rho_k, P_k^j) \geq E_{th,k}. \end{aligned} \tag{12}$$

In each subproblem, all constraints only limit the interval of ρ_k and the objective function is the logarithm function that is concave and monotonically increases. Therefore, we can solve all subproblems independently with the method applied in the single-device WPBC case. Finally, we obtain the power splitting radio vector $\boldsymbol{\rho} = [\rho_1, \rho_2, \ldots, \rho_N]$.

C. Power Allocation Optimization

At iteration j ($j \geq 1$), given a backscatter time allocation vector $\boldsymbol{\beta}^j$ and a power splitting ratio vector $\boldsymbol{\rho}^j$, the power allocation vector $\mathbf{P}$ can be optimized by solving the following problem

$$\begin{aligned} \max_{\mathbf{P}} \quad & \min\ \beta_k^j \log(1+\gamma_{r,k}({\rho_k}^j, P_k)) \\ \text{s.t.} \quad & C_k^s(\rho_k^j, P_k) \geq C_{th,k}, \quad k=1,\ldots,N \\ & E_k({\beta_k}^j, \rho_k^j, P_k) \geq E_{th,k}, \quad k=1,\ldots,N \\ & \sum_{k=1}^{N} {\beta_k}^j P_k \leq \bar{P}. \end{aligned} \tag{13}$$

The problem in Eq. (13) is non-convex, since all constraint functions $C_k^s(\rho_k^j, P_k)$ are non-convex with respect to P_k and coupled with each other. To handle the non-convex constraints, we exploit the SCA method to approximate the logarithm function with its upper estimate function. Since the logarithm function is concave, it can be globally upper-bounded by its linear upper bound approximate at any point (i.e., first order Taylor expansion). Therefore, we can have the following concave lower bound at a local point P_k^{j-1}, the power allocation vector in the previous iteration,

$$\begin{aligned} & C_k^s(\rho_k^j, P_k) \geqslant \tilde{C}_k^s(\rho_k^j, P_k) = \\ & \log(1+\gamma_{r,k}({\rho_k}^j, P_k)) + \\ & \log([\mu|h_k|^2|h_{ke}|^2 + |h_{re}|^2](1-\rho_k^j)P_k + |h_{ke}|^2\sigma_k^2 + \sigma_e^2) - \\ & \{\log(|h_{re}|^2(1-\rho_k^j)P_k^{j-1} + \mu|h_k|^2|h_{ke}|^2 + |h_{ke}|^2\sigma_k^2 + \sigma_e^2) \\ & + \frac{|h_{re}|^2(1-e_k^j)(P_k - P_k^{\{j-1\}})}{|h_{re}|^2(1-\rho_k^j)P_k^j + \mu|h_k|^2|h_{ke}|^2 + |h_{ke}|^2\sigma_k^2 + \sigma_e^2}\}, \end{aligned} \tag{14}$$

where the last two items in braces are the the upper bound of the logarithm function. With the lower bound function in Eq. (14), by introducing a lower-bound minimum throughput $\tilde{R}$ as a slack variable, the problem in Eq. (13) is approximated as the following

$$\begin{aligned} \max_{\mathbf{P}} \quad & \tilde{R} \\ \text{s.t.} \quad & \beta_k^j \log(1+\gamma_{r,k}({\rho_k}^j, P_k)) \geq \tilde{R}, \quad k=1,\ldots,N \\ & \tilde{C}_k^s(\rho_k^j, P_k) \geq C_{th,k}, \quad k=1,\ldots,N \\ & E_k({\beta_k}^j, \rho_k^j, P_k) \geq E_{th,k}, \quad k=1,\ldots,N \\ & \sum_{k=1}^{N} {\beta_k}^j P_k \leq \bar{P}. \end{aligned} \tag{15}$$

The problem (15) is a convex optimization problem that can be solved efficiently with CVX. And more importantly, the lower bound function adopted in Eq. (15) implies that its feasible set is always a subset of that of the problem in Eq. (13). The solution to the problem in Eq. (15) is also a feasible solution to the problem in Eq. (13) [22]. As a result, the maximal objective value obtained from the problem in Eq. (15) is a lower bound of the one in Eq. (13).

Algorithm 1. Overall iterative algorithm for solving problem (8)

1: Initialize $\boldsymbol{\beta}^0$, $\boldsymbol{\rho}^0$,$\mathbf{P}^0$. Set $j=0$ and a small threshold constant $\varepsilon > 0$.
2: **repeat**
3: Set $j \leftarrow j+1$.
4: Obtain the optimal solution $\boldsymbol{\beta}^j$ by solving the problem (10) under given $\boldsymbol{\rho}^{j-1}$ and $\mathbf{P}^{j-1}$.
5: Obtain the optimal solution $\boldsymbol{\rho}^j$ by solving the problem (11) under given $\boldsymbol{\beta}^j$ and $\mathbf{P}^{j-1}$.
6: Obtain the optimal solution $\mathbf{P}^j$ by solving the problem (13) under given $\boldsymbol{\beta}^j$ and $\boldsymbol{\rho}^j$.
7: **until** The fractional increase of the objective value of problem (8) is smaller than a threshold ε.
8: Return the optimal solution $\boldsymbol{\beta}^j$, $\boldsymbol{\rho}^j$ and $\mathbf{P}^j$

D. Overall Algorithm

By applying the BCD technique, we summarize Algorithm 1 for problem (8), which cyclically and iteratively solve the problems in Eqs. (10), (11) and (13) until it converges. In each iteration, we optimize one of the three block variables while keeping the other two fixed. The obtained solution in each iteration is used as the input of the next step.

E. Convergence and Complexity Analysis

For the classic BCD method with cyclic block coordinate descent, the search along with any block coordinate direction is required to yield a unique optimal solution so as to guarantee the convergence [22]. However, in Algorithm 1, for the power allocation subproblem, we only solve its approximate problem optimally. Thus, we need to prove the convergence of our algorithm as the original problem.

The max-min problem in Eq. (8) can be converted to maximize a slack variable R that is smaller than all $R_{r,k}(\rho_k, \beta_k, P_k)$, $\forall k$ [25]. So the Lagrangian for problem in Eq. (8) is given as Eq. (16), where nonnegative vector $\mathbf{a} = [a_1, a_2, \ldots, a_N]^T$, $\mathbf{b} = [b_1, b_2, \ldots, b_N]^T$, $\mathbf{c} = [c_1, c_2, \ldots, c_N]^T$, scale $d \geq 0$ and f are the Lagrange

$$L(\boldsymbol{\beta},\boldsymbol{\rho},\mathbf{P},\mathbf{a},\mathbf{b},\mathbf{c},d,f) =$$
$$R-\sum_{k=1}^{N}a_k(R_{r,k}-R)-\sum_{k=1}^{N}b_k(C_k^s-C_{th,k})-\sum_{k=1}^{N}c_k(E_k-C_{th,k})+d(\sum_{k=0}^{N}\beta_k P_k-\overline{P})+f(\sum_{k=0}^{N}\beta_k-1) \tag{16}$$

Algorithm 2. BSUM algorithm for obtaining Lagrange dual function

1: Find a feasible point $\mathbf{x}^0$ and set j=0. Define a set Γ^j as the block-variable indices at iteration j.
2: **repeat**
3: pick index set Γ^r.
4: let $x_i^j \in \operatorname{argmax} u_i(\mathbf{x}_i,\mathbf{x}^{j-1})$, $i \in \Gamma^j$
5: Set $x_i^j = x_i^{j-1}$, $i \notin \Gamma^j$.
6: $j \leftarrow j+1$.
7: **until** convergence criterion is met

multipliers. Thus Lagrange dual function of the problem is then given by

$$\mathcal{G}(\mathbf{a},\mathbf{b},\mathbf{c},d,f) = \max_{\boldsymbol{\beta},\boldsymbol{\rho},\mathbf{P}} L(\boldsymbol{\beta},\boldsymbol{\rho},\mathbf{P},\mathbf{a},\mathbf{b},\mathbf{c},d,f). \tag{17}$$

The dual problem is thus given by

$$\min_{\mathbf{a},\mathbf{b},\mathbf{c},d,f} \mathcal{G}(\mathbf{a},\mathbf{b},\mathbf{c},d,f). \tag{18}$$

Since the objective is a non-convex function, maximization problem cannot be directly solved by applying the Karush-Kuhn-Tucker (KKT) conditions [22].

For obtaining the Lagrange dual function, we just simplify the Lagrange $L(\boldsymbol{\beta},\boldsymbol{\rho},\mathbf{P})$ without the Lagrange multipliers $\mathbf{a},\mathbf{b},\mathbf{c},d,f$. Based on the BSUM algorithm [23], at the previous iteration feasible point $\mathbf{x}^{j-1}$ ($\mathbf{x}^j \triangleq (\boldsymbol{\beta}^j,\boldsymbol{\rho}^j,\mathbf{P}^j)$), let us select $u_i(\mathbf{x}_i,\ \mathbf{x}^{j-1})$ as an upper bound approximate function of $L(\boldsymbol{\beta},\boldsymbol{\rho},\mathbf{P})$ for each block coordinate i ($i=(j \bmod 3)+1$). At each iteration j, the part C_k^s in the $u_i(\mathbf{x}_i,\ \mathbf{x}^{j-1})$ is replaced by $\tilde{C}_k^s$ if the block variable $\mathbf{P}$ is picked otherwise kept the same. If the $\boldsymbol{\beta}$, $\boldsymbol{\rho}$ and P are alternately selected as x_i, the Algorithm 2 is the same as Algorithm 1. Since each $u_i(\mathbf{x}_i,\ \mathbf{x}^{j-1})$ is continuous and differentiable, each iteration has a unique and regular solution. Based on the Theorem 1 in [23], the sequence $\{\mathbf{x}^j\}_{j=1}^{\infty}$ generated by Algorithm 2 will converge to an accumulation point that is the global optimal solution of Lagrange dual function. With this approach, the multipliers need to be updated iteratively in the external loop to solve the dual problem (18), that leads to double-loop algorithms, requiring more subgradient steps with high complexity.

In addition, in step 4 and step 5 of the Algorithm 1, since both of the subproblems are linear problems and the unique optimal solution can be obtained, we have the following inequality on the objective value

$$R(\boldsymbol{\beta}^j,\boldsymbol{\rho}^j,\mathbf{P}^j) \leqslant R(\boldsymbol{\beta}^{j+1},\boldsymbol{\rho}^{j+1},\mathbf{P}^j). \tag{19}$$

And in the step 6, we can obtain

$$R(\boldsymbol{\beta}^{j+1},\boldsymbol{\rho}^{j+1},\mathbf{P}^j) = \tilde{R}(\boldsymbol{\beta}^{j+1},\boldsymbol{\rho}^{j+1},\mathbf{P}^j)$$
$$\leqslant \tilde{R}(\boldsymbol{\beta}^{j+1},\boldsymbol{\rho}^{j+1},\mathbf{P}^{j+1}) \leqslant R(\boldsymbol{\beta}^{j+1},\boldsymbol{\rho}^{j+1},\mathbf{P}^{j+1}).$$

With the two inequalities, we can further have

$$R(\boldsymbol{\beta}^j,\boldsymbol{\rho}^j,\mathbf{P}^j) \leqslant R(\boldsymbol{\beta}^{j+1},\boldsymbol{\rho}^{j+1},\mathbf{P}^{j+1}), \tag{20}$$

which implies that the objective value of problem in Eq. (8) is non-decreasing. In the above analysis, the sequence $\{\mathbf{x}^j \triangleq (\boldsymbol{\beta}^j,\boldsymbol{\rho}^j,\mathbf{P}^j)\}_{j=1}^{\infty}$ will converge to an stationary point of the problem in Eq. (8). Therefore, the objective value $R(\boldsymbol{\beta}^j,\boldsymbol{\rho}^j,\mathbf{P}^j)$ will converge to an optimal solution and the convergence of the Algorithm 1 is guaranteed. □

For the complexity of Algorithm 1, as numerically shown in Section VI, it converges typically in a few iterations in our simulation setup. In each iteration, since only one LP and one convex optimization problem are solved efficiently by using CVX, the time complexity of each iteration is polynomial. So the complexity of Algorithm 1 is polynomial. Therefore, our algorithm can be practically implemented with fast convergence for a WPBC network with a moderate number of BDs.

VI. Simulation Results

In this section, we provide numerical results to evaluate the performance of the proposed algorithms. In the simulation setup, we considered a WPBC system with N BDs and one eavesdropper that are located in a cell with random distances to the AP. The forward and backward channel gains are set as $10^{-2}d_i^{-2}$, where d_i denotes the distance between the AP and i-th BD. The minimum secrecy rate $\bar{C}_{th}$ and the sum harvested power threshold $\bar{E}_{\min}$ are set to be the same for all users, i.e., $C_{th,k}=\bar{C}_{th}$ and $E_{\min,k}=\bar{E}_{\min}, k=1,\ldots,N$. The total transmission power budget for AP is set to $P=20$ dBm and the receiver noise power is assumed to be σ^2=-60 dBm. Other parameters are set as $\mu=0.6$, $\eta_1=0.6$ and $\eta_2=0.2$.

For performance comparison, we also introduced two cases in the simulation. For the first scheme, denoted as SOA, the eavesdropper was equipped with a single omni-directional antenna. We just considered the artificial noise directly transmitted from AP, because it is typically much large than the backscatter noise power. For the second scheme, the eavesdropper was equipped with a single directional antenna (SDA), only receiving the artificial noise backscattered from BD. We just considered the backscattered artificial noise in this case. As discussed previously, the environmental noise at the eavesdropper is unknown, so we assumed that the worst-case scenario that there is no AWGN noise at the eavesdropper $\sigma_e^2=|h_{ke}|^2\sigma_k^2=0$.

First, Fig. 5 depicts the convergence behavior of the proposed algorithm in two cases, comparing with the global optimal value through exhaustive search. In general, the proposed algorithm achieves the global optimality about 8 iterations within an increment, which is smaller than a set threshold $\varepsilon=10^{-4}$. In addition, we can observe that the max-min throughput in the SOA is larger than the SDA, since the AP needs to split more power for artificial noise in SDA. And

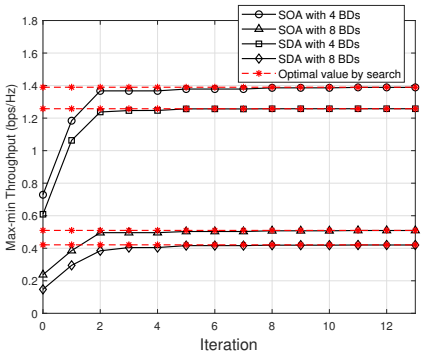

Fig. 5. Convergence behavior of Algorithm 1.

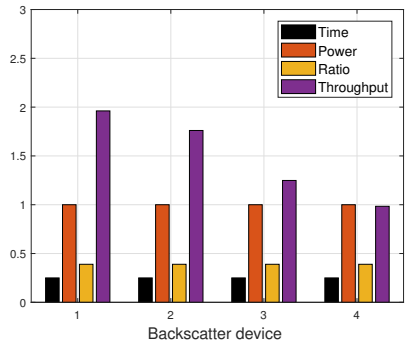

Fig. 6. Throughput with equal resource allocation.

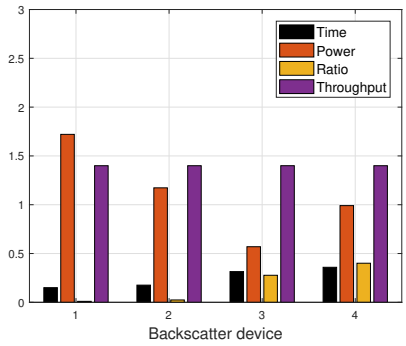

Fig. 7. Throughput with optimal resource allocation.

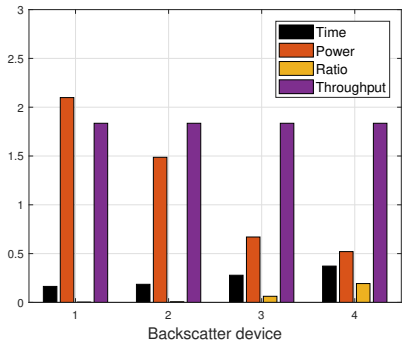

Fig. 8. Throughput with optimal resource alloca -tion with higher total transmission power.

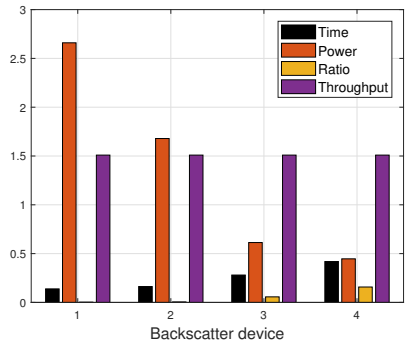

Fig. 9. Throughput with optimal resource alloca -tion with lower secrecy capacity.

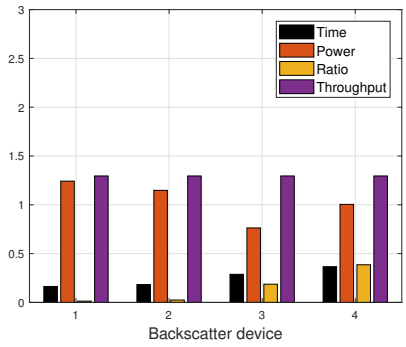

Fig. 10. Throughput with optimal resource alloca -tion with higher harvested energy constraint.

for both 4 BDs and 8 BDs case, there are almost the same convergence speed. But in simulation, the latter needs little more time for CVX to solve the optimization problem in each step, since it have more variables in the problem with more BDs.

Next, we illustrated the whole network performance with different resource allocation policy and system requirements by using a simplified case with $N = 4$ BDs, where the distance of each BD from the AP increases in turn. We mainly focused on the second case that is the worst case in practice, since the eavesdropper can minimize or potentially eliminate the artificial noise directly from the AP. The analysis procedure can also be applicable and suitable to the first case. Fig. 6 depicts the network performance with an equal resource allocation policy for all BDs, and the identical system requirements. From these results, the backscatter throughput of each BD declines one by one, as the distance between the BD and the AP increases. And, the closest BD to the AP, has the highest backscatter throughput than other BDs. With the same augmentation of allocation power for all BDs, there is a greatest throughput increment on the closest BD. If just maximizing the total throughput of all BDs, most of resources will allocated to the closest BD.

After applying our proposed algorithm, each BD has the maximal and identical backscatter throughput with the same system requirements, as shown in Fig. 7. For example, AP assigns more power to the closer devices because of the higher backscatter rate profit. With the higher allocated power, the splitting ratio can be properly decreased, as long as the secrecy capacity is satisfied, and the backscatter time is largely reduced under the same throughput. The saved time can be allocated to the farther BDs and improve their throughput. For the third and fourth device, the eavesdropper is closer to them, so the splitting ratio is suitable but bigger than the closer BDs, which means more power is allocated to the artificial noise to meet the secrecy capacity. But the fourth BD needs more additional power to satisfy the secrecy requirement, because it is farther from the AP and more closer to the eavesdropper.

Then we increased the total power transmitted by the AP to improve the backscatter throughput of all the devices, as shown in Fig. 8. As the total transmission power increases, the resource allocation policy will also be updated to optimize the max-min throughput. Firstly, the power splitting ratios for all BDs are reduced compared to the result in Fig. 7, since higher signal power leads to higher secrecy capacity. Thus, the AP can allocate less power to artificial noise while keeping the same secrecy capacity that can further increase the backscatter rate. Identically, as the higher backscatter rate gain is obtained at the close devices, they will get less backscatter time and more backscatter time is allocated to the far devices. In addition, with higher transmission power, the fourth BD does not need additional power to hold the secrecy capacity.

Fig. 9 demonstrates the system performance and the resource allocation policy with a low secrecy capacity. Compared with Fig. 7, we can observe that with the decrease of the required secrecy capacity, the splitting ratios of all BD are declined and more power are split into the information carrier. Therefore, the max-min throughput of all BDs is improved compared to the backscatter throughput in Fig. 7. In the same way, the fourth BD does not need additional power. In Fig. 10, with a higher harvested energy constraint, the max-min throughput of the system declines compared to the result in Fig. 7, as more power is allocated to the far devices to keep the harvested energy satisfying with the requirement, such as the device 3 and 4. But with the same transmission power and the same secrecy capacity, as shown in Fig. 7, the fourth BD also needs more additional power to satisfy the secrecy requirement. From the analysis of the above cases, under satisfying the security and fairness among all BDs, the closer BDs will be allocated with more transmission power while the farther BDs with more transmission time.

VII. Conclusion

This study investigated the optimization policy for joint backscatter time and power allocation, as well as power splitting ratio selection for securing uplink, in a multi-user WPBC network. We formulated the optimization problem to maximize the minimum throughput while satisfying the requirements on secrecy capacity and harvested energy. The performance of the single-BD WPBC system was theoretically analyzed and evaluated by proof-of-concept experiments. Then, we presented an efficient iterative algorithm to solve the non-convex joint optimization problem of the multi-BDs WPBC network, where the convergence can be guaranteed. Numerical simulation results show that the optimal throughput for all BDs can be fairly achieved, and our work can provide a good perspective of system resource allocation in terms of different limitations and requirements in multi-user WPBC.

Acknowledgment

This work is supported in part by US National Science Foundation NSF under grants CNS-1619073 and CNS-1464487, the National Natural Science Foundation of China (grant 61672410), the Academy of Finland (grant 308087) and the China 111 project (grant B16037).

References

[1] T. D. P. Perera, D. N. K. Jayakody, S. K. Sharma, S. Chatzinotas, and J. Li, "Simultaneous wireless information and power transfer (SWIPT): Recent advances and future challenges," *IEEE Communications Surveys & Tutorials*, vol. 20, no. 1, pp. 264–302, Dec. 2017.

[2] C. Boyer and S. Roy, "Backscatter communication and RFID: Coding, energy, and MIMO analysis," *IEEE Transactions on Communications*, vol. 62, no. 3, pp. 770–785, Mar. 2014.

[3] K. F. Han and K. B. Huang, "Wirelessly powered backscatter communication networks: Modeling, coverage, and capacity," *IEEE Transactions on Wireless Communications*, vol. 16, no. 4, pp. 2548–2561, Sep. 2017.

[4] X. Chen, D. W. K. Ng, and H.-H. Chen, "Secrecy wireless information and power transfer: challenges and opportunities," *IEEE Wireless Communications*, vol. 23, no. 2, pp. 54–61, Apr. 2016.

[5] G. Yang, C. K. Ho, and Y. L. Guan, "Multi-antenna wireless energy transfer for backscatter communication systems," *IEEE Journal on Selected Areas in Communications*, vol. 33, no. 12, pp. 2974–2987, Dec. 2015.

[6] B. Lyu, Z. Yang, G. Gui, and Y. Feng, "Optimal resource allocation policies for multi-user backscatter communication systems," *Sensors*, vol. 16, no. 12, Nov. 2016.

[7] G. Yang, D. Yuan, Y.-C. Liang, R. Zhang, and V. C. M. Leung, "Optimal resource allocation in full-duplex ambient backscatter communication networks for wireless-powered IoT," *arXiv preprint arXiv:1806.06598*, May 2018.

[8] B. Clerckx, Z. B. Zawawi, and K. B. Huang, "Wirelessly powered backscatter communications: Waveform design and SNR-energy tradeoff," *IEEE Communications Letters*, vol. 21, no. 10, pp. 2234–2237, Oct. 2017.

[9] B. Clerckx, "Wireless information and power transfer: Nonlinearity, waveform design and rate-energy tradeoff," *IEEE Transactions on Signal Processing*, vol. 66, no. 4, pp. 847–862, Feb. 2018.

[10] H. Xing, L. Liu, and R. Zhang, "Secrecy wireless information and power transfer in fading wiretap channel," *IEEE Transactions on Vehicular Technology*, vol. 65, no. 1, pp. 180–190, Jan. 2016.

[11] L. Liu, R. Zhang, and K.-C. Chua, "Secrecy wireless information and power transfer with MISO beamforming," *IEEE Transactions on Signal Processing*, vol. 62, no. 7, pp. 1850–1863, Dec. 2014.

[12] D. W. K. Ng, E. S. Lo, and R. Schober, "Robust beamforming for secure communication in systems with wireless information and power transfer," *IEEE Transactions on Wireless Communications*, vol. 13, no. 8, pp. 4599–4615, Aug. 2014.

[13] W. Saad, X. Y. Zhou, Z. Han, and H. V. Poor, "On the physical layer security of backscatter wireless systems," *IEEE Transactions on Wireless Communications*, vol. 13, no. 6, pp. 3442–3451, Jun. 2014.

[14] J. Granjal, E. Monteiro, and J. S. Silva, "Security for the Internet of Things: A survey of existing protocols and open research issues," *IEEE Communications Surveys & Tutorials*, vol. 17, no. 3, pp. 1294–1312, Jan. 2015.

[15] P. Zhang, J. Gummeson, and D. Ganesan, "Blink: A high throughput link layer for backscatter communication," in *Proceedings of the 10th International Conference on Mobile Systems, Applications, and Services (MobiSys'12)*. New York, USA: ACM, 2012, pp. 99–112.

[16] M. Zhang and Y. Liu, "Energy harvesting for physical-layer security in OFDMA networks," *IEEE Transactions on Information Forensics and Security*, vol. 11, no. 1, pp. 154–162, Jan. 2016.

[17] M. S. Trotter, J. D. Griffin, and G. D. Durgin, "Power-optimized waveforms for improving the range and reliability of RFID systems," in *IEEE International Conference on RFID*, Orlando, USA, Apr. 2009, Conference Proceedings, pp. 80–87.

[18] A. Collado and A. Georgiadis, "Optimal waveforms for efficient wireless power transmission," *IEEE Microwave and Wireless Components Letters*, vol. 24, no. 5, pp. 354–356, May 2014.

[19] H. Ju and R. Zhang, "Throughput maximization in wireless powered communication networks," *IEEE Transactions on Wireless Communications*, vol. 13, no. 1, pp. 418–428, Jan. 2014.

[20] W.-C. Liao, T.-H. Chang, W.-K. Ma, and C.-Y. Chi, "QoS-based transmit beamforming in the presence of eavesdroppers: An optimized artificial-noise-aided approach," *IEEE Transactions on Signal Processing*, vol. 59, no. 3, pp. 1202–1216, Mar. 2011.

[21] J. R. Smith, *Wirelessly powered sensor networks and computational RFID*. New York, USA: Springer Science & Business Media, 2013.

[22] D. G. Luenberger and Y. Ye, *Linear and nonlinear programming*. Reading, MA: Springer, 2016.

[23] M. Hong, M. Razaviyayn, Z.-Q. Luo, and J.-S. Pang, "A unified algorithmic framework for block-structured optimization involving big data: with applications in machine learning and signal processing," *IEEE Signal Processing Magazine*, vol. 33, no. 1, pp. 57–77, Jan. 2016.

[24] A. Beck, A. Ben-Tal, and L. Tetruashvili, "A sequential parametric convex approximation method with applications to nonconvex truss topology design problems," *Journal of Global Optimization*, vol. 47, no. 1, pp. 29–51, May 2009.

[25] S. Boyd and L. Vandenberghe, *Convex optimization*. Cambridge, UK: Cambridge university press, 2004.

[26] M. Grant and S. Boyd, "CVX: Matlab software for disciplined convex programming, version 2.1," Mar. 2014.